Bull Volcanol
DOI 10.1007/s00445-012-0646-5

RESEARCH ARTICLE

The 5,660 yBP Boquerón explosive eruption, Teide–Pico Viejo complex, Tenerife

Olaya García · Costanza Bonadonna · Joan Martí · Laura Pioli

Received: 5 March 2012 / Accepted: 28 July 2012

Abstract Quantitative hazard assessments of active volcanoes require an accurate knowledge of the past eruptive activity in terms of eruption dynamics and the stratified products of eruption. Teide–Pico Viejo (TPV) is one of the largest volcanic complexes in Europe, but the associated eruptive history has only been constrained based on very general stratigraphic and geochronological data. In particular, recent studies have shown that explosive activity has been significantly more frequently common than previously thought. Our study contributes to characterization of explosive activity of TPV by describing for the first time the subplinian eruption of El Boquerón (5,660 yBP), a satellite dome located on the northern slope of the Pico Viejo stratovolcano. Stratigraphic data suggest complex shifting from effusive phases with lava flows to highly explosive phase that generated a relatively thick and widespread pumice fallout deposit. This explosive phase is classified as a subplinian eruption of VEI 3 that lasted for about 9–15 h and produced a plume with a height of up to 9 km above sea level (i.e. 7 km above the vent; MER of 6.9–8.2 × 10^5 kg/s). The tephra deposit (minimum bulk volume of 4–6 × 10^7 m^3) was dispersed to the NE by up to 10 m/s winds. A similar eruption today would significantly impact the economy of Tenerife (e.g. tourism and aviation), with major consequences mainly for the communities around the Icod Valley, and to a minor extent, the Orotava Valley. This vulnerability shows that a better knowledge of the past explosive history of TPV and an accurate estimate of future potentials to generate violent eruptions is required in order to quantify and mitigate the associated volcanic risk.

Keywords Teide · Explosive volcanism · Tephra deposits · Hazard assessment

Editorial responsibility: S. De la Cruz-Reyna

O. García (✉)
Centro Geofísico de Canarias del I.G.N.,
C/La Marina 20, 2°,
Q1 38001 Santa Cruz de Tenerife, Spain
e-mail: ogperez@fomento.es

C. Bonadonna · L. Pioli
Département de Minéralogie, Section des sciences de la Terre et de l'environnement, Université de Genève,
Rues des Maraichers 13,
Q2 1205 Geneva, Switzerland

J. Martí
Instituto de Ciencias de la Tierra Jaume Almera, CSIC,
Lluis Solé Sabarís s/n,
08028 Barcelona, Spain

Introduction

The Holocene explosive volcanic activity in Tenerife Island is concentrated mainly in the central volcanic complex (Ablay et al. 1998; Ablay and Martí 2000; Martí et al. 2008).

This central complex started to grow at about 4.5 Ma, or earlier, and remains active. Its evolution included several constructive and destructive episodes that gradually formed Las Cañadas caldera at the centre of the island (Martí et al. 1994; Ancochea et al. 1999). The last episode in the construction of the Tenerife central volcanic complex formed the Teide and Pico Viejo stratovolcanoes (TPV complex) within Las Cañadas caldera (Ablay and Martí 2000; Carracedo et al. 2007). Traditionally considered as mainly effusive volcanoes, current knowledge of TPV remains poor given that they form one of the main active volcanic complexes in Europe and are a significant threat to Tenerife (Martí et al. 2011; Marrero et al. 2012). Recent studies have revealed that explosive activity has been underestimated in the reconstructed TPV eruptive history (Martí et al. 2008, 2011; García et al. 2011; Boulesteix et al. 2012). This implies that hazards at Tenerife might be underestimated if explosive volcanism from TPV is not considered. No precise data on the products of TPV explosive volcanism exist, however, and one of the most urgent needs is to characterise and quantify these eruptions.

The knowledge we have of explosive volcanism at TPV is restricted to a detailed study of the 2,000 BP Montaña Blanca subplinian eruption (Ablay et al. 1995; Folch and Felpeto 2005) and the identification of new fallout and PDC deposits on the northern flank of TPV (Perez-Torrado et al. 2004; Martí et al. 2008; García et al. 2011). Even this limited information suggests that an explosive eruption from TPV would today have a serious impact on critical infrastructures and the economy of the island as it would affect the air traffic, and some of the main energy and water lifelines (Martí et al 2011; Marrero et al. 2012). In this paper, we present a detailed study of the pumice fall deposits associated with El Boquerón dome complex, one of the Holocene flank vents located on the north of the Pico Viejo stratovolcano (Fig. 1). These deposits form the main unit produced by the El Boquerón explosive eruption and have not been described before. We infer the eruption characteristics (i.e. plume height, erupted volume, mass eruption rate and duration) based on a stratigraphic and textural analysis and discuss implications for associated hazards.

Geological background

The TPV complex consists of two stratovolcanoes which started to grow simultaneously within Las Cañadas caldera at around 180–190 ka (Hausen 1956; Araña 1971; Ablay 1997; Ablay et al. 1998; Ablay and Martí 2000; Carracedo et al. 2007) (Fig. 2). This volcanic depression originated as a result of several vertical collapses of the former Tenerife central volcanic edifice, Las Cañadas edifice (Martí et al. 1997; Martí and Gudmundsson 2000). The TPV complex has a maximum elevation of 3,718 m above sea level at the top of Teide and shows a very sharp morphology characterised by steep flanks. The eruptive activity of TPV produced about 150 km^3 of mafic, intermediate and felsic material (Ablay et al. 1998; Ablay and Martí 2000; Martí et al. 2008).

TPV stratovolcanoes have been very active during the Holocene, with more than 16 known eruptions (Carracedo et al. 2007; Martí et al. 2011), the last (Lavas Negras) having occurred at 1,150 yBP (Fig. 2).

The volcano stratigraphy of the TPV was characterized by Ablay and Marti (2000) based on a detailed field and

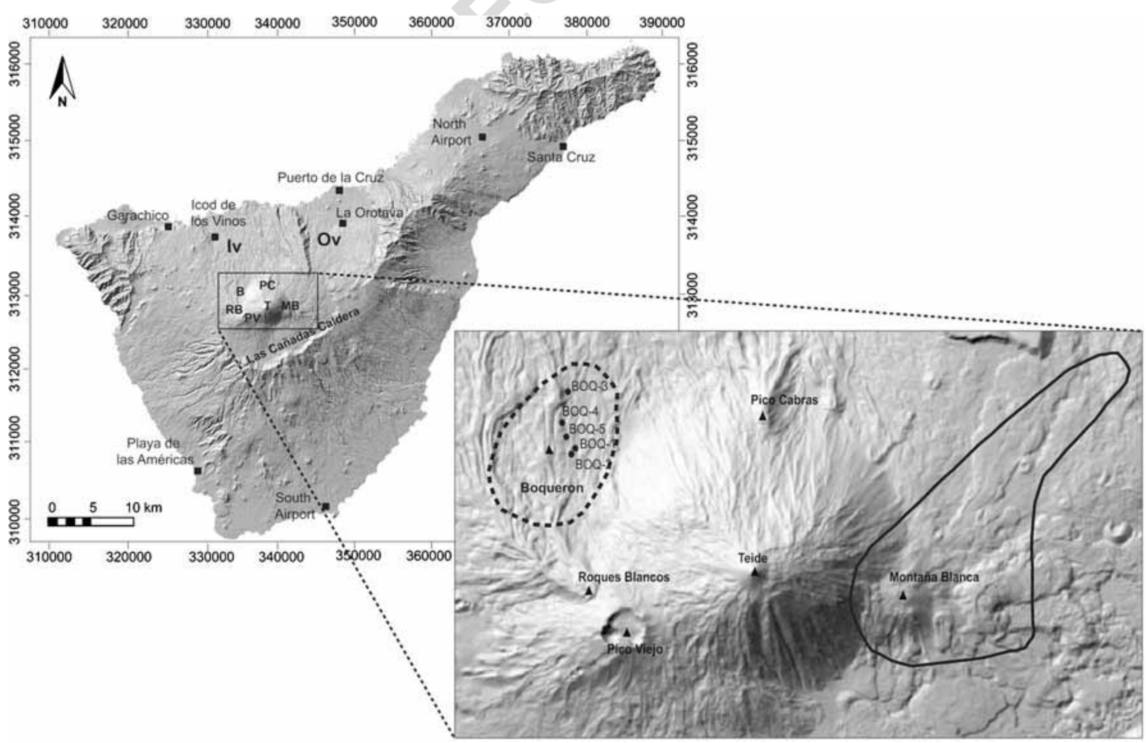

Fig. 1 Location map of study area and topographic map of Tenerife. Main vents and main drainage cuts of Boquerón lava flow are shown as *black triangles* and *black solid lines*, respectively. *Black circles* indicate our main outcrops (Fig. 2), the *dashed line* represents the 50-cm isopach contour of isopach A (Fig. 3) and the *thick line* represents the 30-cm isopach contour. *B* Boquerón, *MB* Montaña Blanca, *RB* Roques Blancos, *T* Teide, *PC* Pico Cabras, *PV* Pico Viejo, *Iv* Icod Valley, *Ov* Orotava Valley (projection: UTM 28 N)

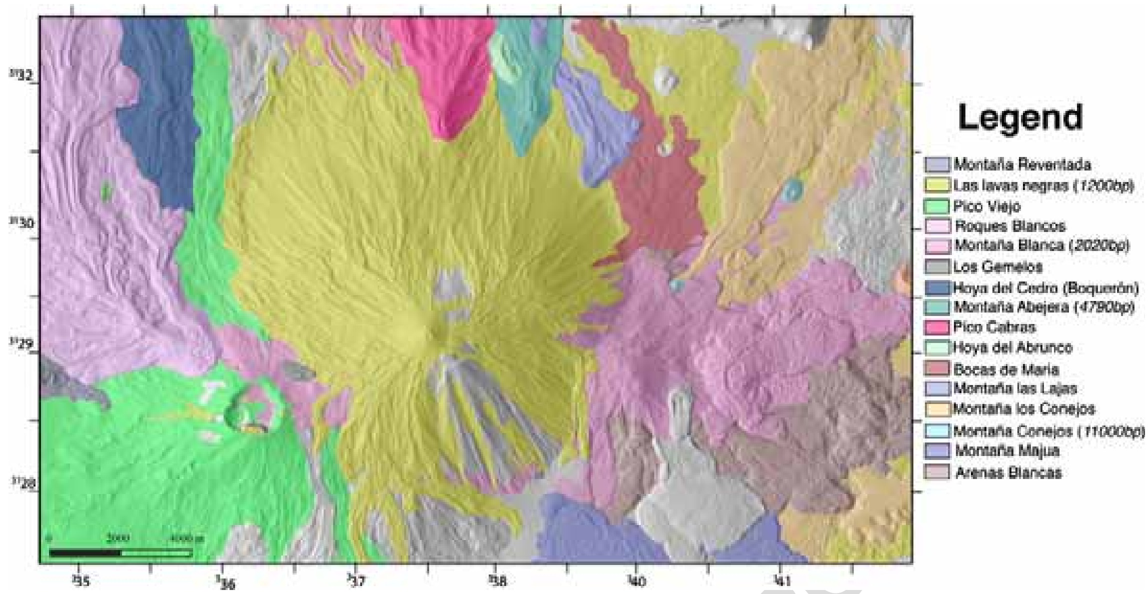

Fig. 2 Geological map of the Teide–Pico Viejo complex; adapted from Ablay and Martí (2000). The figure does not include all the volcanic events related to Pico Viejo–Teide stratovolcanoes, only those central and flank Holocene eruptions with felsic and hybrid composition. Geochronological data from Carracedo et al. (2003, 2007)

petrological study (Fig. 2). In addition, Carracedo et al. (2003, 2007) provided the first group of isotopic ages from TPV products. The eruptive history of TPV consists of a main stage of eruption of mafic to intermediate lavas that form the core of the stratovolcanoes and filled most of the Las Cañadas depression and the adjacent La Orotava and Icod valleys. Phonolitic eruptions have become predominant since 35 ka, and their products cover the volcanoes' flanks and the infill sequence of the Icod Valley and part of La Orotava valley (Fig. 1).

Phonolitic eruptions from TPV were generated both from the central vents and from a multitude of vents distributed around their flanks. The flank vents define several radial eruptive fissures on the slopes of the twin volcanoes, and have generated both effusive (i.e. lava flows and domes) and explosive eruptions, ranging in size from 0.01 to >1 km^3 Dense Rock Equivalent (DRE). Effusive eruptions have produced thick lava flows and domes. Explosive eruptions have generated extensive pumice fall deposits and pyroclastic density currents (PDCs) associated with both subplinian and plinian eruptions and also with dome and lava flow gravitational collapses in the cases of PDCs (Martí et al. 2008, 2011; García et al. 2011). All these eruptive centres are associated with a single eruption in which several phases may be distinguished (Ablay and Martí 2000).

The Boquerón is a dome complex located on the northwestern flank of TPV volcano. The last Boquerón eruption is of Holocene age (Carracedo et al. 2003) and produced both a large pumice fall deposit and 0.04 km^3 of lava flows, which reached the coastline along the Icod valley (i.e. 7.2 km run out; Fig. 1; Martí et al. 2011). In this paper, we present a detailed study of the fall deposit.

Methods

Given the poor exposure of the Boquerón deposit, the relevant outcrops were first identified based on aerial photographs and then thoroughly analysed and correlated through field investigations. Most of the studied outcrops are located on the northwest flank of TPV, at the base of Roques Blancos dome complex, and are concentrated in a 15-km^2 area around Boquerón (Fig. 1). The stratigraphy of the whole sequence of deposits was characterised based on detailed fieldwork. Correlations among the different units from different outcrops were made mainly based on textural features and crystal content and composition. Deposit thickness and maximum lithic sizes were determined at most outcrops. Forty samples were also collected in order to investigate grain size, chemistry, density and vesicularity of the juvenile pumices. The fraction coarser than $-3\ \phi$ (i.e. >8 mm) was sieved manually in the field, whereas finer fractions >3 ϕ (<8 mm) were dried and sieved in the laboratory. Componentry analysis was made for particles coarser than 0 ϕ.

Density was measured on 100 juvenile clasts from the entire unit, collected at the outcrop BOQ-4 and with diameters ranging between 16 and 32 mm (Fig. 3). Pumice clasts were dried at 60 °C for 24 h and then cleaned with a brush, numbered and weighed. Finally, all clasts were coated with

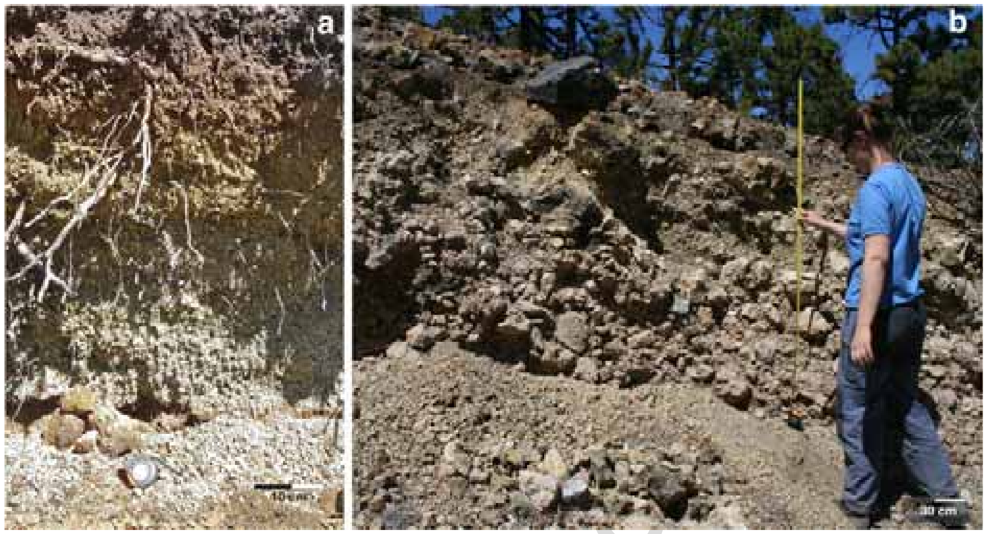

Fig. 3 Pumice fall deposit from the Boquerón eruption. **a** Distal area: outcrop BOQ-3A. **b** Proximal area of pumice deposit with a large lithics: outcrop BOQ-2.TOP

cellulose acetate, dried and weighed again. Relative density was obtained comparing water and the dry weights. The results were converted into absolute density and bulk vesicularity using the Dense Rock Equivalent (DRE) density measured on finely crushed pumice specimens using a water pycnometer at the University of Geneva. The deposit density in the field was obtained by weighing a known in situ volume of pumice clasts, plus intergranular porosity and matrix from BOQ-3 outcrop. To investigate variations in morphology and vesicularity of juvenile clasts of the main unit, we used the scanning electron microscope (SEM) JEOLJSM 6400 at the University of Geneva.

Whole rock analyses were performed by the GeoAnalytical Laboratory at the Washington State University using X-ray fluorescence (XRF) and inductively coupled plasma mass spectrometry (ICP-MS) facilities. The relative error of the measurement is lower than 1 % for the major and trace elements for XRF method, less than 5 % for the REEs and less than 10 % for the remaining trace elements. Charcoal was also found in the soil below the bottom unit of Boquerón deposit, which overlies the paleosol, and 2.2 g of sample was analyzed by Beta Analytic Inc. Laboratory of Miami (USA) for carbon isotopic composition with accelerator mass spectroscopy (AMS) techniques. The specimen (i.e. laboratory number Beta-298872) age was determined after the IntCal04 calibration curve (Reimer et al. 2004).

Physical parameters of the main unit were also derived. The erupted volume was calculated applying the methods of exponential, power-law and Weibull integration (Pyle 1989; Bonadonna and Houghton 2005; Bonadonna and Costa 2012). Given the poor exposure of the deposits, two potential isopach maps were compiled based on the same dataset in order to investigate the uncertainty in the volume calculation. The thickness dataset was constructed based on 61 trenches excavated down to the underlying lava flow (in medial areas) or down to a maximum of 2 m when the lava flow was not present (in proximal areas).

The plume height was determined applying the method of Carey and Sparks (1986) to the isopleth map of lithic clasts. The maximum lithic sizes were measured based on the geometric mean average of the three axes of the five largest clasts sampled based on a horizontal sampling area of 0.5 m^2. We also compiled an isopleth map using the 50th percentile of the 20 largest clasts following the recommendations of the IAVCEI Commission on Tephra Hazard Modelling (Bonadonna et al. 2011, 2012).

Composition, stratigraphy and characteristics of deposits

The Boquerón eruption is associated with an old dome in the northwest flank of Pico Viejo stratovolcano. Charcoal fragments found in the dark red soil at the base of Boquerón deposit had a 13C/12C ratio of −22.9‰, corresponding to a conventional age of 5,630±60 yBP, corresponding to a calibrated radiocarbon age of 5,660±60 BP. The composition (shown in Table 1) of both the Boquerón juvenile fragments and lava flow is phonolitic, similar to other Holocene products of TPV (see Ablay et al. 1995).

The pyroclastic succession of the Boquerón deposit consists of a main pumice fall deposit characterised by a poor exposure, with proximal outcrops showing some evident stratification and some welding phenomena (Fig. 3). Individual layers are difficult to correlate and tend to merge in distal areas. As a result, we have characterised the Boquerón deposit as a single unit. Five representative outcrops were selected for detailed stratigraphic, grain size, componentry and textural studies and are shown in Fig. 4.

The Boquerón tephra deposit is dispersed over an area of about 15 km^2 NW of Teide. In distal areas (Fig. 2; BOQ-3), it consists of several centimetre-thick, well-sorted, non-

Table 1 Whole rock analyses of representative Boquerón samples

Unit sample	Boquerón Boq.r23	Boquerón Boq.r1	Boquerón Boq.pr
Major and minor elements (oxides, wt.%)			
SiO_2	59.46	58.44	59.14
TiO_2	0.727	0.63	0.70
Al_2O_3	19.34	18.9	19.44
FeO^*	3.45	3.51	3.41
MnO	0.19	0.19	0.19
MgO	0.43	0.34	0.38
CaO	0.87	0.75	0.76
Na_2O	8.92	9.07	9.08
K_2O	5.50	5.42	5.59
P_2O_5	0.114	0.081	0.070
Total	99.0	97.33	98.77
LOI (%)	0.89	2.35	0.87
Trace elements (ppm)			
Ni	4	3	4
Cr	2	2	2
Sc	0	1	1
V	14	8	13
Ba	192	24	87
Rb	169	170	186
Sr	13	7	10
Zr	964	989	1,041
Y	36	38	38
Nb	219	225	235
Ga	28	29	29
Cu	1	1	2
Zn	119	125	125
Pb	19	20	20
La	110	112	112
Ce	186	186	192
Th	28	28	30
Nd	55	56	57
U	7	8	7

Q5 Boq.r23 is a lava from a Boquerón lava flow; it was taken from one point close to point 6 (Table 2), and Boq.r1 and Boq.pr are juvenile lapilli clasts and were taken from no-welded bed at point 4 (Table 2)

welded, massive bed of pumice lapilli. Grain size distribution of the studied samples is characterised by Md phi and sorting varying between −1.4 and −3.2 phi and 1.4 and 1.0, respectively. Lithic content is mostly constant for all deposits, increasing slightly from the bottom (7 vol.%) to the top (10 vol.%; Fig. 4); lithic clasts predominantly consist of obsidian and phonolitic lava fragments. Juvenile clasts consist of microvesicular, crystal-poor, angular to subangular yellow to grey pumice lapilli. At medial locations (Fig. 4; BOQ-2), the unit has a thickness of a few decimetres and displays internal stratification with symmetric, coarse–fine–coarse graded bedding. The contact between beds is gradational. At proximal locations (Fig. 4; BOQ-5 and BOQ-2), the deposit consists of an alternation of moderately to incipiently welded lapilli and bomb beds and non-welded lapilli beds with exposed thickness up to 6.37 m (outcrop BOQ-5). These layers are moderately to poorly sorted, with average size from lapilli to bombs. In the welded beds, the degree of welding increases from bottom to top with gradual transition to the lower non-welded beds. The welded beds are typically lithic-poor. At some locations, the welded beds display rheomorphic features suggesting remobilization on steep slopes. The welding of the proximal deposits suggests higher deposition rates and high depositional temperatures associated with low magma viscosity, favouring clast agglutination and deformation (Carey et al. 2008). This appears to be a common process in the phonolitic eruptions of the TPV complex, and also affected the older plinian fall deposits cropping out in the Las Cañadas walls (Ablay et al. 1995; Soriano et al. 2002).

In contrast, the contact between non-welded layers is sharp (Fig. 4; BOQ-4). The bottom of the whole unit lies over a paleosol or, in distal areas, directly above lava flows. Carracedo et al. (2003) located the vent of this eruption at the S margin of the lava flow. This hypothesis is confirmed by the distribution of thickness and grain size of the tephra layer (Fig. 5 and Table 2).

Results

Volume

In order to estimate the error associated with the volume calculation of a poorly exposed tephra deposit, we decided to hand draw two possible isopach maps based on the same dataset (isopach maps A and B in Fig. 5 with associated thickness shown in Table 2). Map A is compiled based on a conservative interpretation of field data, while Map B can be considered as just an example of possible contouring that can be drawn to consider a larger dispersal than Map A but still compatible with the same dataset. In fact, Map B is compiled based on the assumption of a more gradual thinning where the deposit is not accessible (i.e. mainly to the SW and NE of the vent) and can be then considered as an upward boundary for the volume calculation (with a relative difference of 30 % in the square root of area value of the 50-cm contour). The thinning trends resulting from each map can be described by one exponential segment and both a Weibull and a power-law curve on a semi-log plot of thickness versus square root of isopach area.

Volume calculations were then made from the two different maps applying the methods of exponential, power-law and Weibull integrations (Pyle 1989; Bonadonna and

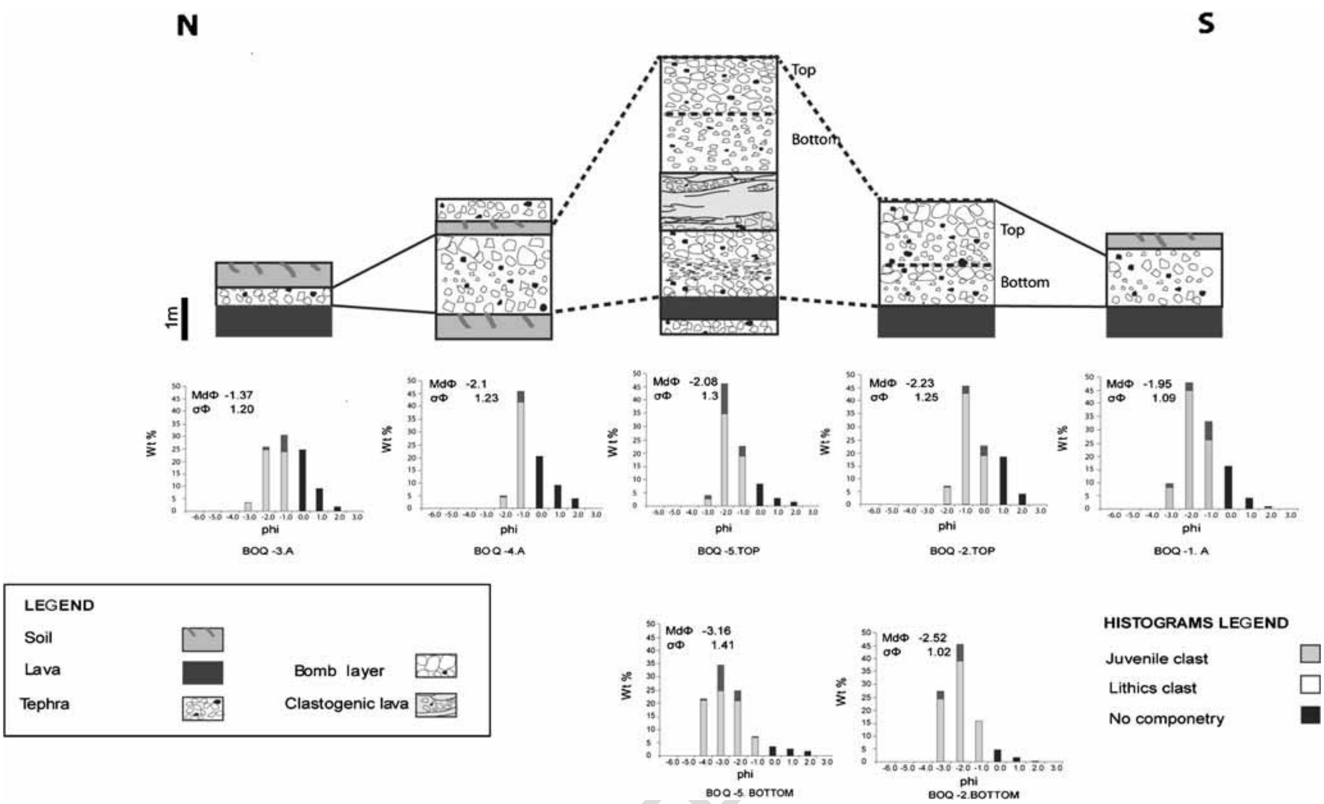

Q6 **Fig. 4** Stratigraphic columns of five representative sections from Boquerón deposits with the associated grain size and componentry. Location of the outcrops is shown in Fig. 1 and thickness in Table 2

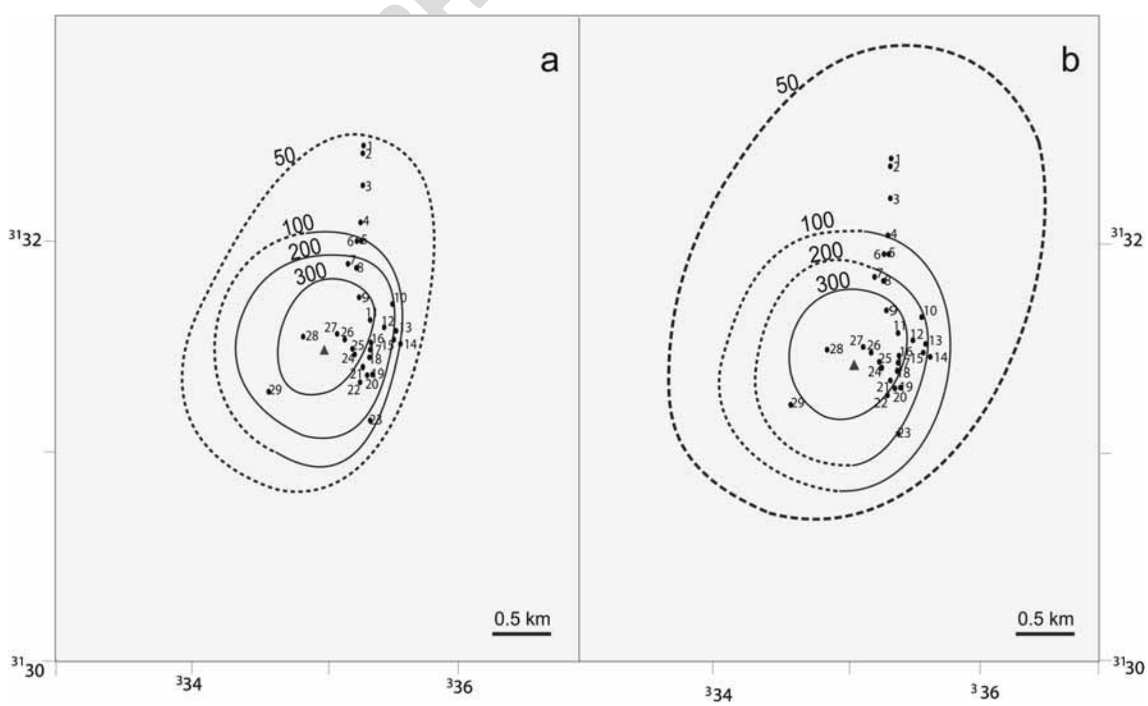

Fig. 5 Isopach maps of the Boquerón deposit with thickness expressed in centimetre: (**a**) isopach map A; (**b**) isopach map B. Sample numbers are indicated on the map, and thickness values are reported in Table 1. *Dashed lines* are extrapolated contours. Given the poor exposure of the deposit, two isopach maps have been compiled that are compatible with our dataset in order to estimate the error in the volume calculation

Table 2 Thickness values of samples points in isopach maps A and B of Fig. 3

Point	Thickness (cm)	UTM X	UTM Y
1	60	335356	3132377
2	62	335356	3132337
3	**40**	**335328**	**3132052**
4	37	335314	3131765
5	58	335312	3131620
6	50	335285	3131609
7	**164**	**335288**	**3130977**
8	>120	335225	3131436
9	**637**	**335311**	**3131145**
10	>79	335636	3131111
11	>120	335416	3130977
12	>165	335546	3130946
13	>79	335655	3130878
14	110	335698	3130773
15	>140	335636	3130811
16	**271**	**335437**	**3130789**
17	>180	335416	3130722
18	>188	335402	3130645
19	>112	335426	3130531
20	>197	335390	3130520
21	>140	335340	3130583
22	>99	335315	3130456
23	>180	335412	3130163
24	>160	335266	3130698
25	>185	335254	3130733
26	>180	335172	3130816
27	**>160**	**335092**	**3130857**
28	>165	334801	3130818
29	>200	334463	3130400

Numbers in bold show the thickness of the main outcrops; *Point 3* is BOQ-3

Houghton 2005; Bonadonna and Costa 2012; Table 3). The calculated volumes are 1.0 and 1.7×10^{7} m^3 for the two exponential integrations, $3.7\pm0.4\times10^{7}$ and $7.3\pm1.2\times10^{7}$ m^3 for the two power-law integrations and 4.2×10^{7} and 6.3×10^{7} m^3 for the two Weibull integrations (for isopach A and B respectively; Fig. 5). The erupted mass varies between 0.6 and 4.4×10^{10} kg based on a deposit density of 600 kg m^{-3}. The distal limits of integration for the power-law calculation (50 to 100 km square root of area values; Table 3) were chosen based on both the thinning trend of Boquerón and Montaña Blanca (Ablay et al. 1995). In fact, these two deposits show very similar features with a thickness of about 10–50 cm around 3–5 km from the vent (square root of area values). We assume that the most distal sedimentation would then occur around 50 to 100 km from the vent (square root of area values). The error of the power-law integration was calculated based on the variation of these distal integration limits. The uncertainty associated with the compilation of the isopach map is 40 % for exponential method, 50 % for the power-law method and 32 % for the Weibull method. As a result, we base our discussion below on the most stable values given by the Weibull integration. The associated DRE volume, based on a deposit density of 600 kg/m^3 and a magma density of 2,570 kg/m^3, ranges from 9.9×10^{6} to 1.5×10^{7} m^3.

Plume height, wind speed, mass eruption rate and eruption duration

As mentioned above, two isopleth maps were compiled based on the five largest lithics (Fig. 6a) and on the 50th percentile of a population of 20 lithics (Fig. 6b). Plume height and wind velocity at the time of the eruption were derived by applying the method of Carey and Sparks (1986) to both isopleth maps. Only the 0.8-cm isopleth contour gave consistent estimates for both maps, and resulted in a plume height of about 7 km above the vent (i.e. about 9 km above sea level) for both the five largest clasts and the 50th percentile method and wind velocities up to 10 m/s. The Boquerón tephra deposit was mainly dispersed northeastward, in agreement with the dominant wind direction in the area. In fact, the average wind direction in TPV complex, as calculated based on NOAA local wind data collected in the last 10 years, shows a dominant eastward wind direction from 5 to 20 km above sea level with uniform seasonal distribution and standard deviation decreasing from ±90° to ±45° with altitude (Fig. 7).

The mass eruption rate (MER) was calculated applying both the method of Wilson and Walker (1987) and Sparks (1986) (Table 4). The method of Wilson and Walker (1987) resulted in a MER of 6.9×10^{5} kg/s, while the method of Sparks (1986) resulted in a MER of 8.2×10^{5} kg/s (for a tropical atmosphere and a plume temperature of 600 °C appropriate for phonolitic magmas). The eruption duration was estimated between about 9–10 h for isopach A and about 13–15 h for isopach B based on the ratio between erupted mass (Weibull integration) and the two MER values described above (Table 4).

Classification

Based on the volume range described above, the Boquerón explosive phase classifies as having a volcanic explosivity index (VEI) of 3. The associated magnitude is between 2.8 and 3.6, and the intensity is 9 on the scales of Pyle (2000) (Table 3). The bt vs. bc/bt plot of Pyle (1989) suggests an eruptive style between strombolian and subplinian, with the subplinian field being characterised by minimum plume heights of 14 km (Fig. 8). The thinning trend, however,

Table 3 Summary of volume calculations associated with the exponential (Pyle 1989), power-law (Bonadonna and Houghton 2005) and Weibull (Bonadonna and Costa 2012) integrations

		Volume (×10^{7} m^{3})	Mass (×10^{10} kg)	Magnitude		
					bt (km)	bc/bt
Exponential	Isopach A	1.0	0.6	2.8	2.0	0.3
	Isopach B	1.7	1.0	3.0	1.3	0.4
					m	
Power law	Isopach A	3.7±0.4	2.2±0.3	3.3	1.8	–
	Isopach B	7.3±1.2	4.4±0.7	3.6	1.6	–
					θ	*λ*
Weibull	Isopach A	4.2	2.5	3.4	4.7	13.8
	Isopach B	6.3	3.8	3.6	5.5	18.1

Mass is calculated based on a deposit density of 600 kg/m^3; magnitude is calculated according to Pyle (2000); bt and bc are the thickness half-distance and the half-distance ratio, respectively, calculated according to Pyle (1989); *m* is the absolute value of the coefficient of the power-law best fit; *θ* and *λ* are two characteristic scales of the Weibull best fit. The error of the power-law integration is calculated based on variable distal limits of integrations (i.e. 50, 75 and 100 km)

follows the typical pattern of subplinian eruptions and, in particular, shows similar characteristics to that of the Montaña Blanca deposit (Fig. 9). Values of thickness half distance (bt) for Boquerón maps A and B are between 0.3 and 0.5 km in agreement with bt values of Montaña Blanca deposit (i.e. 0.4–0.8 km), of the 26 September 1997 vulcanian explosion of Montserrat (i.e. 0.7 km), of Chaiten layer α (i.e. 0.7 km) and with the proximal bt values of Ruapehu (i.e. 0.2 km) and Chaiten layer β (i.e. 0.8 km). These values are lower than values of Plinian eruptions that typically range from 1 to 60 km (Pyle 1989).

Clast vesicularity and textural characterization

The phenocryst content of the Boquerón pumices account for 3 to 7 vol.%. Phenocrysts consist of millimetre-sized, euhedral biotite, alkaline feldspar, clinopyroxene and minor apatite, magnetite and ilmenite.

Juvenile lapilli are usually microvesicular, glassy and phenocryst poor. The differences between juvenile clasts can be substantial, both in density and texture (Figs. 10 and 11). Their density ranges from 360 to 1,150 kg/m^3 with average of 744 kg/m^3 and standard deviation of 190 kg/m^3

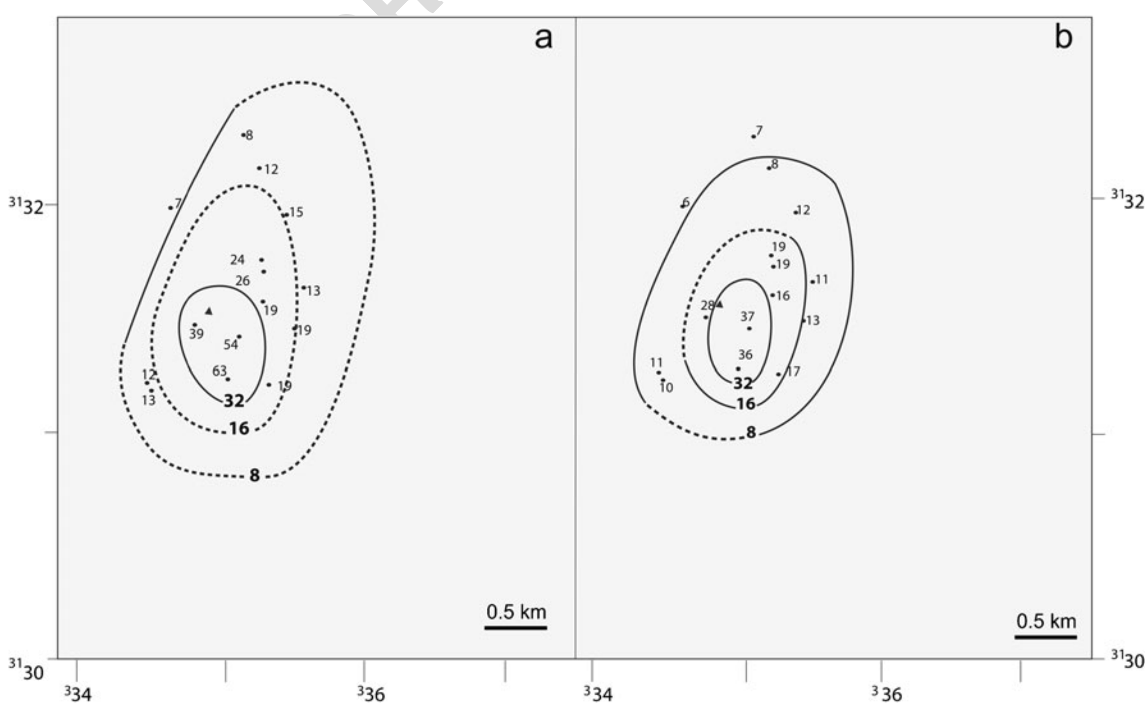

Fig. 6 Isopleth maps of Boquerón deposit for the largest lithics using two different methods: (**a**) the average of the three axes of the five largest clasts; (**b**) 50th percentile of a 20-clast population. *Dashed lines* are extrapolated contours

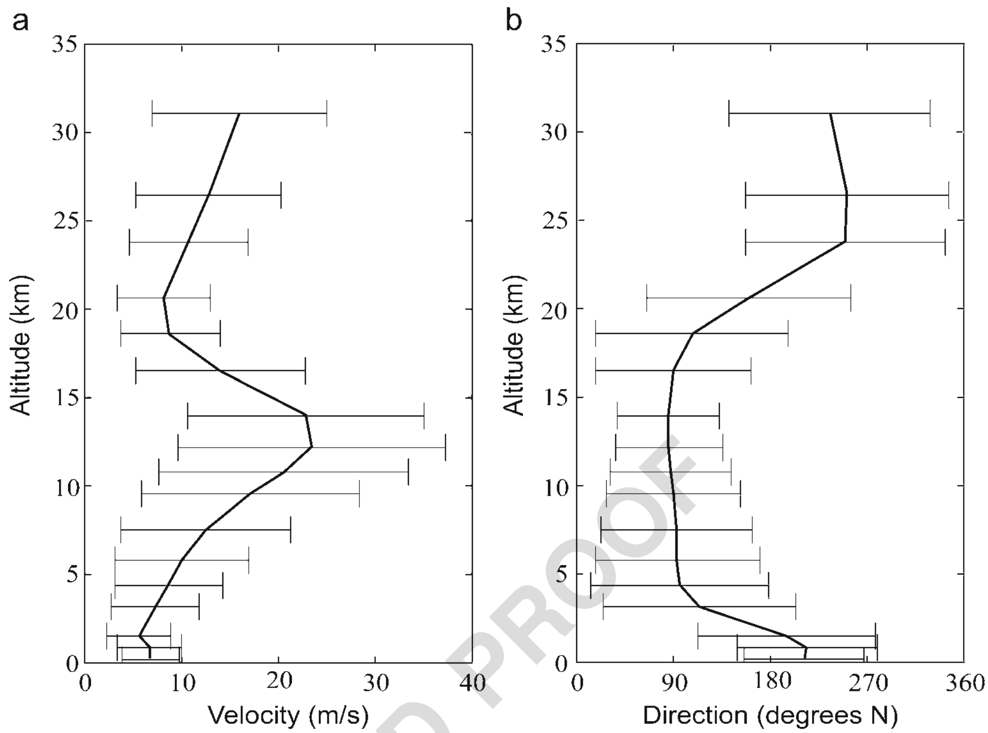

Fig. 7 Wind profiles calculated for Teide–Pico Viejo Volcano for the last 10 years (2000–2010; wind data from NOAA, US National Oceanic and Atmospheric Administration, www.cdc.noaa.gov). **a** Variation of wind velocity profile with altitude. **b** Variation of wind direction, which is expressed as degrees from north where the wind blows. Data are presented as a median value with associated *error bars*

(Fig. 10). The density distribution is unimodal with a dense tail. Considering a measured DRE density of 2,540±133 kg/m^3, the vesicularity ranges from 86 to 33 vol.%, and the clasts could be classified as from poorly to highly vesicular (Houghton and Wilson 1989).

Vesicles range from a few millimetres to few micrometres in size and display different shapes, from spherical to elongate or flat (Fig. 10a). The largest vesicles have complex and irregular shapes (Fig. 10a). The majority of clasts display homogenous textures with high vesicularity, small vesicles with complex shapes and glassy groundmass (Fig. 10b), and vesicle walls thickness ranges from few micrometres to a few tens of micrometres, suggesting high nucleation rates, and an expansion dominated coalescence (Szramek et al. 2006).

Moderately to poorly vesicular clasts have heterogeneous textures, with vesicularity and crystallinity varying at the millimetre scale. Vesicles are separated by thicker (a few tens to few hundreds of micrometres) walls (Fig. 11d) and cluster in groups. Larger vesicles are usually confined to the central portion of the clasts. In addition, groundmass crystallinity varies at the specimen scale and is correlated with the vesicularity: microlite-poor areas (5 vol.% of microlites) are also vesicle-poor, with only small round vesicles; microlite-rich areas (50 vol.% of microlites) have vesicularity up to 45 vol.%. This relationship between vesicles and groundmass crystallinity is possibly due to the effects of post-fragmentation expansion or even by clast recycling during lower explosivity phases (Wright et al. 2006). The boundaries between microlite-poor areas and microlite-rich areas are generally sharp (Fig. 11b).

Microlites consist of acicular sanidine with major axes ranging between 200 and 10 μm. Occasionally, microlites are gathered in small groups in the crystal-rich glass, but it is more common to see individual crystals. Clasts from incipiently welded facies show highly heterogeneous textures with abrupt variations in vesicles size and spherulitic aggregates.

Table 4 Summary of the MER and eruption duration calculation based on a plume height of 6.8 km (calculated with the method of Carey and Sparks 1986) and for the methods of Wilson and Walker (1987) and Sparks (1986)

	MER ($\times10^5$ kg/s)	Duration (isopach A) (h)	Duration (isopach B) (h)
Wilson and Walker (1987)	6.9	10.2	15.1
Sparks (1986)	8.2	8.6	12.7

The eruptions duration is calculated based on the ratio between the erupted mass (calculated based on the Weibull integration applied to isopach A and B of Fig. 3) and the two values of MER

Discussion

The Boquerón subplinian eruption produced a vigorous plume reaching up to 9 km above sea level. The wind dispersion was to the Northeast in agreement with the main wind pattern of the area and with the dispersion of the Montaña Blanca eruption (Ablay et al. 1995; Folch and Felpeto 2005). Despite the low column height, the

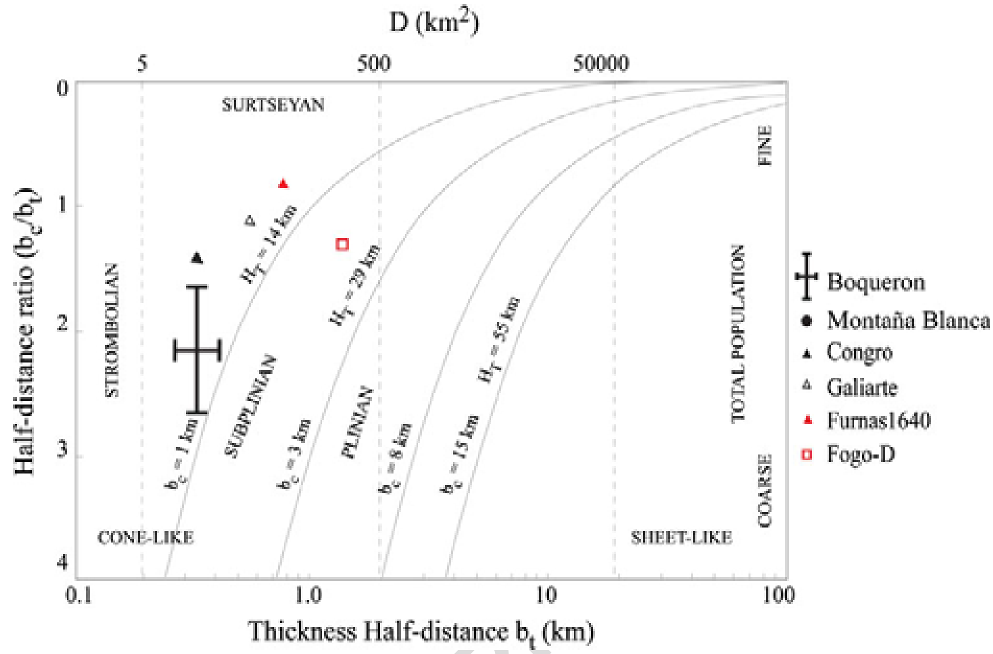

Fig. 8 Classification plot of Pyle (1989). Boquerón data are indicated as median value with associated *error bar*. *Error bar* is calculated based on the two isopach maps of Fig. 3. Data of Congro, 3,800 yBP, Sao Miguel, Azores (Booth et al. 1978); Furnas 1640, Sao Miguel, Azores (Thorinsson and Sigvaldson 1972a, b); Fogo D, Cape Verde (Rose et al. 1983) and Montaña Blanca, 2 Ka Tenerife (Ablay et al. 1995) eruptions are also shown for comparison

Boquerón eruption is also comparable to other subplinian events in terms of deposit dispersal, erupted volume and thinning trend (Fig. 9). As an example, the Boquerón volume and thinning trends are very similar to those for the eruptions of Montaña Blanca (i.e. 1.4×10^8 m^3 based on isopach map from Ablay et al. 1995) and Fuego 1974 (Rose et al. 2008). The complex stratigraphy, which is evident at proximal locations, could be indicative of complex eruption dynamics, coupling a main climactic phase to minor explosive phases that formed the welded horizons in the deposit, or to fluctuations in the eruptive intensity. Finally, we note that our new radiometric data suggest a maximum age for the Boquerón eruption of 5,660 yBP. This age is much older, but compatible with the value (2,528±185 yBP) obtained by

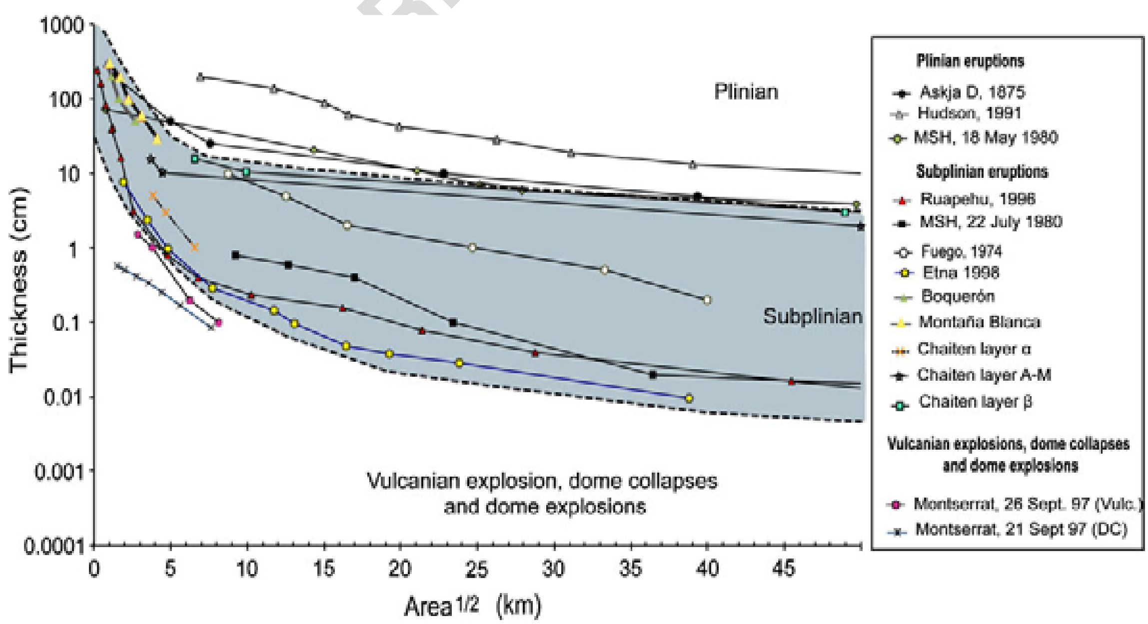

Fig. 9 Semi-log plot of thickness versus the square root of the area of the Boquerón deposit compared with the thinning trend of other deposits produced by explosive eruptions. Data are from Askja D, 1875 (Sparks et al. 1981); Hudson, 1991 (Scasso et al. 1994); Mount St. Helens, 18 May 1980 (Sarna-Wojcicki et al. 1981); Ruapehu, 17 June 1996 (Bonadonna and Houghton 2005); Montserrat, 26 September 1997 (Bonadonna et al. 2002); Montserrat, 21 September 1997 (Bonadonna et al. 2002); Fuego, 1974 (Rose et al. 2008); Etna, 1998 (Bonadonna and Costa 2012); Montaña Blanca, 2 Ka (Ablay et al. 1995); and Chaiten, May 2008 (Alfano et al. 2010)

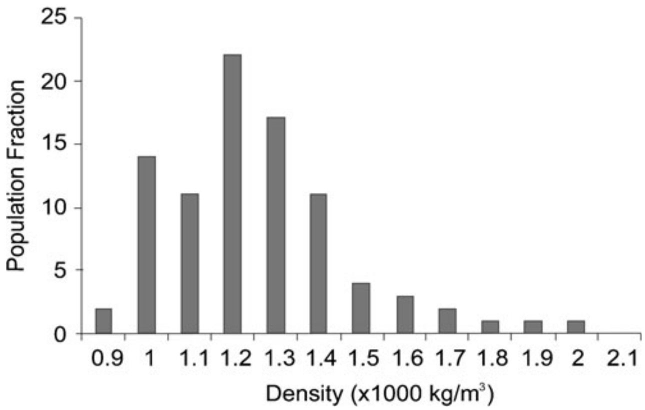

Fig. 10 Density distribution histogram of juvenile clasts from Boquerón unit

Carracedo et al. (2007) from a charcoal in the paleosol. Both ages are consistent with the regional stratigraphy (Ablay and Martí 2000).

Deposit dispersal, eruption column and duration

In order to estimate the uncertainty involved in calculating the volumes of deposits characterised by poor exposure, we constructed two possible isopach maps based on the same set of data. The error associated with the two compilations of the isopach map is about 30 %, 40 % and 50 % for Weibull, the exponential and the power-law method, respectively. These values are of the same order of magnitude of other estimations of volume-calculation uncertainties made on better-exposed deposits (e.g. 30 % estimated uncertainty for the exponential method by Cioni et al. (2011) on the 512 AD Vesuvius eruptions). In addition, Bonadonna and Costa (2012) have already shown how the stability of the Weibull method is better than that of the other two empirical methods because it depended on only three free parameters (i.e. λ, θ, and n). As a result, the volume can be constrained more easily (when ≥3 points are available) and without the need of arbitrary and subjective choices, such as the number of exponential segments and the integration limits.

The plume height was derived using the method of Carey and Sparks (1986). In particular, the height derived based on the average of geometric mean of the five largest clasts was compared to the height derived based on the 50th percentile of a 20-clast population suggested by the IAVCEI Commission on Tephra Hazard Modelling (Bonadonna et al. 2011; Bonadonna et al. 2012). In fact, the method of the 50th percentile is considered more stable even though it still needs to be calibrated with the original plots of Carey and Sparks (1986). As a result, we confidently conclude that the plume reached a maximum height of 7 km above the vent (i.e. 9 km above sea level). The uncertainty in the calculation of the MER based on two different methods is around 16 % (Wilson and Walker 1987; Sparks 1986), which results

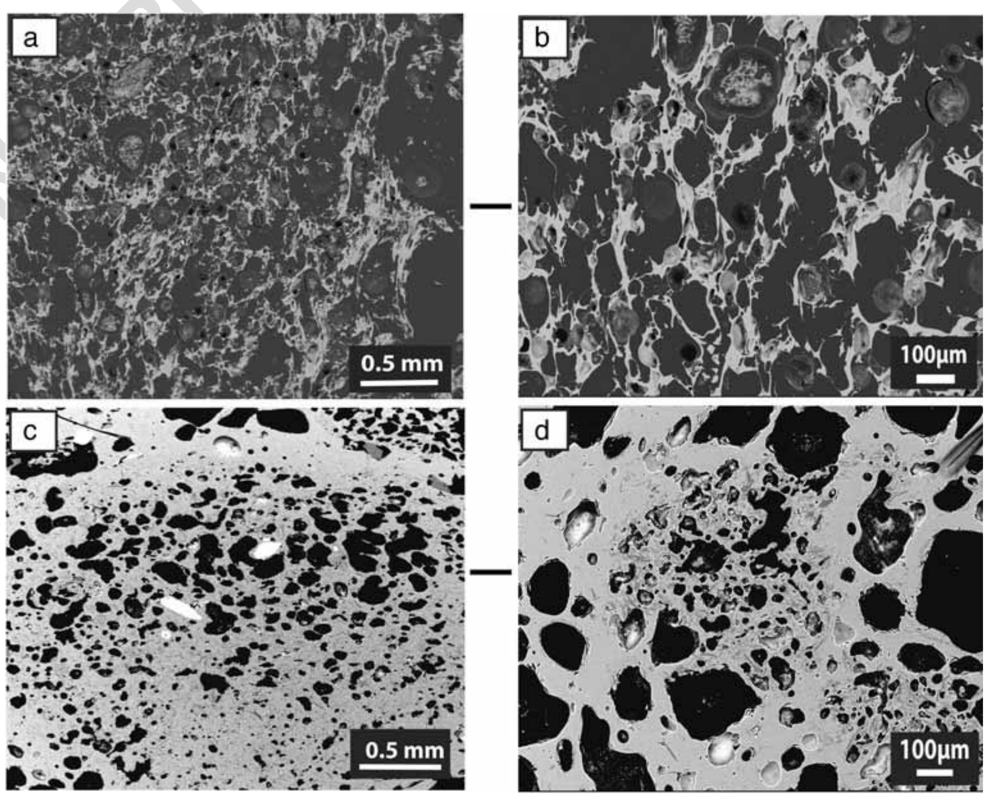

Fig. 11 Selected backscattered SEM images (×25 and ×200 magnification) of juvenile clasts of different vesicularity. Vesicles are in *black*, while the glass and microlites groundmass are in *grey*. **a** Sample with high vesiculation. **b** Detail of vesicles in the sample with high vesiculation. **c** Sample with low vesiculation. **d** Detail with vesicles in the sample of low vesiculation

in an uncertainty in the inferred eruption duration of up to 43 % based on the two MER values and the Weibull-derived volume associated with isopach maps A and B (Table 4).

Textures

Boquerón juvenile pumice fragments have been characterised on the basis of vesicularity and groundmass texture. The differences between juvenile clasts can be substantial, both in density and texture (Figs. 10 and 11). The majority of clasts display homogenous textures with high vesicularity, small vesicles with complex shapes and glassy groundmass, suggesting high nucleation rates, and an expansion-dominated coalescence (Szramek et al. 2006). In contrast, the lower vesicularity clasts display heterogeneous textures with smaller, rounded vesicles and higher groundmass crystallinity, possibly due to the effects of post-fragmentation expansion and clasts recycling during lower explosivity phases (Wright et al. 2006). In addition, the welding of the proximal deposits suggests higher deposition rates and high depositional temperatures associated with low viscosity, favouring clast agglutination and deformation (Carey et al. 2008). This appears to be a common process for phonolitic eruptions of the TPV complex, and for older plinian fall deposits cropping out in the Las Cañadas walls (Ablay et al. 1995; Soriano et al. 2002).

Volcanic hazard and risk

TPV is one of the largest volcanic complexes in Europe and is located at the top of a densely populated island that is also a very popular destination for tourism. The main known volcanic hazard is associated with basaltic fissural eruptions, which mainly take place along the two active rift zones. However, there is also clear evidence of effusive and explosive phonolitic volcanism during the Holocene, with significant hazard implications, not only for the Las Cañadas area but also for the Icod valley, which connects the TPV complex to the N coast of the island. In fact, among the known lateral eruptions of the TPV complex, at least 16 have produced phonolitic magmas, which can also be associated with highly mobile, low-viscosity lava flows (Dingwell et al. 1998; Giordano et al. 2000; Gottsmann and Dingwell 2001). Like the Boquerón, most of these eruptions were also dome forming with vents located at the flanks of the TPV (2,300 m above sea level), and they also had associated PDCs (Martí et al. 2008, 2011). Among them, the Montaña Blanca (2,020 BP) is the best known and most recent eruption (Ablay et al. 1995). It produced a 10-km high eruption column and a tephra deposit with a volume of 1.4×10^{8} m^3 dispersed over an area of 30 km^2 (based on maps of Ablay et al. 1995). The last eruption in Tenerife was the basaltic strombolian eruption of Chinyero, 1909, on the NW rift, which did not cause major disruption to population (Solana and Aparicio 1998). The only known eruption that has caused fatalities and major disruption in Tenerife occurred in 1706, when a basaltic lava flow, originated from a vent on the Santiago rift (outside the TPV), almost destroyed Garachico, the former capital of the island, inducing a massive spontaneous evacuation (Solana and Aparicio 1998). Since then, Tenerife has experienced population growth significantly higher than the national average, and it is now the most populated island of Spain with more than 900,000 inhabitants. In addition, Tenerife is one of the main tourist destinations in Europe with more than five million visitors per year, and the main populated municipalities in Tenerife (Santa Cruz, San Cristobal de la Laguna and Puerto de la Cruz) are less than 30 km away from the TPV. Aviation could also be significantly affected by a new explosive eruption of the TPV. In fact, all Canarias airports fall in a circle of 300 km radius centred on the TPV complex, with the Canary Islands lying along one of the main civil aviation corridors for flights from Europe to Central and South America and vice versa. Martí et al. (2011) have already shown that a subplinian eruption from the Boquerón vent (i.e. calculations based on a plume height of 9 km above sea level and volume of 0.05 km^3) would significantly affect the Northern coast of Tenerife, including the towns of Icod de los Vinos, Santa Cruz, La Orotava, Puerto de la Cruz and the North airport. All the roads in the northern part of the island and the main road that connects the North to the South would be covered by 1 mm to 5 cm of ash. Given that our detailed study of the Boquerón eruption results in a similar plume height and volume as modelled by Martí et al. (2011) (i.e. 7 km and 0.04–0.06 km^3 respectively), we would expect that another eruption of this type would be associated to disruption equivalent to that described by Martí et al. (2011).

Conclusions

Despite poor levels of exposure, we have provided an accurate study of the deposits associated with the last Boquerón eruption based on a detailed description of stratigraphy and sedimentological features, including the morphology, textural features and composition of the juvenile fraction. This has allowed for a reconstruction of the eruption dynamics and the main physical parameters. As a result, we can conclude that

1. Empirical calculations resulted in a tephra volume between 1 and 8×10^{7} m^3 with the best estimate between 4 and 6×10^{7} m^3 (based on the Weibull integration of two possible maps). The uncertainty associated with the volume calculation of tephra deposits is about 30 %,

40 % and 50 % for the Weibull, exponential and the power-law integrations, respectively.

2. The plume reached a maximum height of 9 km above sea level (i.e. 7 km above the vent) with a corresponding MER and duration of 6.9–8.2 $\times 10^5$ kg/s and 9–15 h, respectively.
3. The explosive phase could be classified as a VEI=3 subplinian eruption based on dispersal and thinning characteristics. Magnitude and intensity are 3.4–3.6 and 9, respectively.
4. The proximal welding and stratification of the deposit, together with the typical pumiceous textures of the majority of the lapilli, suggest complex dynamics, shifts from highly explosive phases to minor phases, and dispersal high temperature bombs in proximal locations.
5. If a Boquerón-style eruption were to happen again, it would have a large impact on the now densely populated island of Tenerife, particularly towards the north, and on various economic sectors, such as the aviation business.

Acknowledgments This research has been partially funded with MICINN grant CGL2008-04264 and the IGN-CSIC collaboration agreement for the study of Tenerife volcanism. The authors are grateful to the National Park of Teide for giving us permission to undertake this research and Cabildo of Tenerife for giving us FYF 412/10 permission. They are also grateful to David Moure, Dario Pedrazzi, Ilazkiñe Iriberren, Natividad Luengo, Stavros Meletlidis, Pedro Torres, Stephanie Barde-Cabusson, Victor Cabrera and all the staff working at the Geophysics Centre of Canarias for their support during the field campaigns, including the staff working in the Central Geophysics Observatory (IGN). They also thank Agathe Martignier of the Department of Mineralogy of University of Geneva (Switzerland) for assistance with the SEM analyses, and Sebastien Biass helped in processing the NOAA wind data. This paper greatly benefited from editorial handling by S. De la Cruz and careful reviews of two anonymous reviewers.

References

Ablay GJ, Martí J (2000) Stratigraphy, structure, and volcanic evolution of the Pico Teide-Pico Viejo formation, Tenerife, Canary Islands. J Volcanol Geotherm Res 103:175–208. doi:10.1016/s0377-0273(00)00224-9

Ablay GJ, Carroll MR, Palmer MR, Martí J, Sparks RSJ (1998) Basanite- phonolite lineages of the Teide-Pico Viejo volcanic complex, Tenerife, Canary Islands. J Petrol 39:905–936

Ablay GJ (1997) Evolution of the Teide-Pico Viejo complex and magma system, Tenerife, Canary Islands. Dissertation. University of Bristol, Bristol

Ablay GJ, Ernst GGJ, Martí J, Sparks RSJ (1995) The 2 ka subplinian eruption of Montaña Blanca, Tenerife. Bull Volcanol 57:337–355

Alfano F, Bonadonna C, Volentik ACM, Connor CB, Watt SFL, Pyle DM, Connor LJ (2010) Tephra stratigraphy and eruptive volume of the May, 2008, Chaitén eruption, Chile. Bull Volcanol 73:613–630. doi:10.1007/s00445-010-0428-x

Ancochea E, Huertas MJ, Fuster JM, Cantagrel JM, Coello J, Ibarrola E (1999) Evolution of the Cañadas edifice and its implications for the origin of the Cañadas caldera (Tenerife, Canary Islands). J Volcanol Geotherm Res 88:177–199

Araña V (1971) Litología y estructura del edificio Cañadas, Tenerife (Islas Canarias). Est Geol 27:95–135

Bonadonna C, Cioni R, Pistolesi M, Connor CB, Scollo S, Pioli L (2012) Determination of the largest clasts of tephra deposits for the characterization of explosive eruptions: report of the IAVCEI Commission on Tephra Hazard Modelling. Bull Volcanol (submitted). https://vhub.org/resources/870

Bonadonna C, Costa A (2012) Estimating the volume of tephra deposits: a new simple strategy. Geology 40:415–418. doi:10.1130/G32769.1

Bonadonna C, Scollo S, Cioni R, Pioli L, Pistolesi M (2011) Determination of the largest clasts of tephra deposits for the characterization of explosive volcanic eruptions. Report of the IAVCEI Commission on Tephra Hazard Modelling

Bonadonna C, Houghton BF (2005) Total grain size distribution and volume of tephra-fall deposits. Bull Volcanol 67:441–456. doi:10.1007/s00445-004-0386-2

Bonadonna C, Macedonio G, Sparks RSJ (2002) Numerical modelling of tephra fallout associated with dome collapses and vulcanian explosions: application to hazard assessment on Montserrat. In: Druitt TH, Kokelaar BP (eds) The eruption of Soufrière Hills Volcano, Montserrat, from 1995 to 1999. Geological Society of London, London, pp 517–537

Booth B, Croasdale R, Walker GPL (1978) A quantitative study of five thousand years of volcanism on Sao Miguel, Azores. Phil Trans R Soc London A288:271–319

Boulesteix T, Hildenbrand A, Soler V, Gillot PY (2012) Eruptive response of oceanic islands to giant landslides: new insights from the geomorphologic evolution of the Teide-Pico Viejo volcanic complex (Tenerife, Canary). Geomorphology 138:61–73. doi:10.1016/j.geomorph.2011.08.025

Carey R, Houghton B, Thordarson T (2008) Contrasting styles of welding observed in the proximal Askja 1875 eruption deposits I: Regional welding. J Volcanol Geotherm Res 171:1–19. doi:10.1016/j.jvolgeores.2007.11.020

Carey S, Sparks RSJ (1986) Quantitative models of the fallout and dispersal of tephra from volcanic eruption columns. Bull Volcanol 48:109–125

Carracedo JC, Rodríguez-Badiola E, Guillou H et al (2007) Eruptive and structural history of Teide volcano and rift zones of Tenerife, Canary Islands. Geol Soc Am Bull 119:1027–1051. doi:10.1130/B26087.1

Carracedo JC, Paterne M, Guillou H et al (2003) Dataciones radiométricas (14C y K/Ar) del Teide y el rift noroeste, Tenerife, Islas Canarias. Est Geol 59:15–29

Cioni R, Bertagnini A, Andronico D, Cole PD, Mundula F (2011) The 512 AD eruption of Vesuvius: complex dynamics of a small scale subplinian event. Bull Volcanol 73:789–810. doi:10.1007/s00445-011-0454-3

Dingwell DB, Hess KU, Romano C (1998) Extremely fluid behavior of hydrous peralkaline rhyolites. Earth Planet Sci Lett 158:31–38

Folch A, Felpeto A (2005) A coupled model for dispersal of tephra during sustained explosive eruptions. J Volcanol Geotherm Res 145:337–349. doi:10.1016/j.jvolgeores.2005.01.010

García O, Martí J, Aguirre-Díaz G, Geyer A, Iribarren I (2011) Pyroclastic density currents from Teide-Pico Viejo (Tenerife, Canary Islands): implications on hazard assessment. TerraNova 23:220–224. doi:10.1111/j.1365-3121.2011.01002.x

Giordano D, Dingwelll DB, Romano C (2000) Viscosity of a Teide phonolite in the welding interval. J Volcanol Geotherm Res 103:239–245

Gottsmann J, Dingwell DB (2001) Cooling dynamics of spatter-fed phonolite obsidian flows on Tenerife, Canary Islands. J Volcanol Geotherm Res 105:323–342

Hausen H (1956) Contributions to the geology of Tenerife (Canary Islands). Soc Sci Fennicae Comm Phys-Mat 18:254

Houghton B, Wilson CJN (1989) A vesicularity index for pyroclastic deposits. Bull Volcanol 51:451–462

Marrero JM, García A, Llinares A et al (2012) A direct approach to estimating the number of potencial fatalities from an eruption: application to the central volcanic complex of Tenerife Island. J Volcanol Geotherm Res 219–220:33–40. doi:10.1016/j.jvolgeores.2012.01.008

Martí J, Sobradelo R, Felpeto A, García O (2011) Eruptive scenarios of phonolitic volcanism at Teide-Pico Viejo volcanic complex (Tenerife, Canary Islands). Bull Volcanol 74:767–782. doi:10.1007/s00445-011-0569-6

Martí J, Geyer A, Andujar J, Teixó F, Costa F (2008) Assessing the potential for future explosive activity from Teide-Pico Viejo stratovolcanoes (Tenerife, Canary Islands). J Volcanol Geotherm Res 178:529–542. doi:10.1016/j.jvolgeores.2008.07.011

Martí J, Gudmundsson A (2000) The Las Cañadas caldera (Tenerife, Canary Islands): an overlapping collapse caldera generated by magma-chamber migration. J Volcanol Geotherm Res 103:161–173

Martí J, Hurlimann M, Ablay GJ, Gudmundson A (1997) Vertical and lateral collapses in Tenerife and other ocean volcanic islands. Geology 25:879–882

Martí J, Mitjavila J, Araña V (1994) Stratigraphy, structure and geochronology of the Las Cañadas caldera (Tenerife, Canary Islands). Geol Mag 131:715–717

Perez-Torrado FJ, Carracedo JC, Paris R, Hansen A (2004) Descubrimientos de depósitos freatomagmáticos en las calderas septentrionales de estratovolcan Teide (Tenerife, Islas Canarias): relaciones estratigraficas e implicaciones volcánicas. Geotemas 6:163–166

Pyle DM (1989) The thickness, volume and grain size of tephra fall deposits. Bull Volcanol 51:1–15

Pyle DM (2000) Size of volcanic eruptions. In: Sigurdsson H (ed) Encyclopedia of volcanoes. Academic, London, pp 263–269

Reimer PJ, Baillie MGL, Bard E, Bayliss A et al (2004) Radiocarbon 46:1029–1058

Thorinsson S, Sigvaldson GE (1972a) The Hekla eruption of 1970. Bull Volcanol 36:269–288

Rose WI, Self S, Murrow PJ, Bonadonna C, Durant AJ, Ernst GGJ (2008) Nature and significance of small volume fall deposits at composite volcanoes: insights from the October 14, 1974 Fuego eruption, Guatemala. Bull Volcanol 70:1043–1067

Rose WI, Wunderman RL, Hoffman MF, Gale L (1983) A volcanologist's review of atmospheric hazards of volcanic activity: Fuego and Mt St Helens. J Volcanol Geotherm Res 17:133–157

Sarna-Wojcicki AM, Shipley S, Waitt JR, Dzurisin D, Wood SH (1981) Areal distribution thickness, mass, volume, and grain- size of airfall ash from the six major eruptions of 1980. US Geol Surv Prof Pap 1250:577–600

Scasso R, Corbella H, Tiberi P (1994) Sedimentological analysis of the tephra from 12–15 August 1991 eruption of Hudson Volcano. Bull Volcanol 56:121–132

~~Self S (1976) The recent volcanology of Terceira, Azores. J Geol Soc London 132:645–666~~ Q11

Solana MC, Aparicio A (1998) Reconstruction of the 1706 Montaña Negra eruption. Emergency procedures for Garachico and El Tanque, Tenerife, Canary Islands. In: Firth CR, McGuire WJ (eds) Geol Soc London Spec Pub 161, pp 209–216

Soriano C, Zafrilla S, Martí J, Bryan S, Cas R, Ablay G (2002) Welding and rheomorphism of phonolitic fallout deposits from the Las Canadas caldera, Tenerife, Canary Islands. Geol Soc Am Bull 114:883–895

Sparks RSJ (1986) The dimensions and dynamics of volcanic eruption columns. Bull Volcanol 48:3–15

Sparks RSJ, Wilson L, Sigurdsson H (1981) The pyroclastic deposits of the 1875 eruption of Askja, Iceland. Philos Trans R Soc Lond 299:241–273

Szramek L, Gardner J, Larsen J (2006) Degassing and microlite crystallization of basaltic andesite magma erupting at Arenal Volcano, Costa Rica. J Volcanol Geother Res 157:182–201. doi:10.1016/j.volgeores.2006.03.039

Thorinsson S, Sigvaldson GE (1972b) The Hekla eruption of 1970. Bull Volcanol 36:269–288

Wilson L, Walker GPL (1987) Explosive volcanic eruptions—VI. Ejecta dispersal in plinian eruptions: the control of eruption conditions and atmospheric properties. Geophys J R Astr Soc 89:657–679

Wright HMN, Cashman KV, Rosi M, Cioni R (2006) Breadcrust bombs as indicators of vulcanian eruptions at Guagua Pichincha volcano, Ecuador. Bull Volcanol 69:281–300. doi:10.1007/s00445-006-0073-6